Chromosome Research (2008) 16:709–719
DOI: 10.1007/s10577-008-1221-y

General pattern of meiotic recombination in male dogs estimated by MLH1 and RAD51 immunolocalization

E. A. Basheva[1,2], C. J. Bidau[3] & P. M. Borodin[1,2]*
[1]*Russian Academy of Sciences, Siberian Department, Institute of Cytology and Genetics, Novosibirsk 630090, Russia; Tel: +7-383-3332813; Fax: +7-383-3331278; E-mail: borodin@bionet.nsc.ru;* [2]*Department of Cytology and Genetics, Novosibirsk State University, Novosibirsk, Russia;* [3]*Oswaldo Cruz Institute, FIOCRUZ, Rio de Janeiro, Brazil*
**Correspondence*

Received 21 January 2008. Received in revised form and accepted for publication by Herbert Mcgregor 18 March 2008

Key words: Canis familiaris, dog, meiotic recombination, MLH1, RAD51, synaptonemal complex

Abstract

The aim of this study was to estimate a general pattern of meiotic recombination in the domestic dog (*Canis familiaris*) using immunolocalization of MLH1, a mismatch repair protein of mature recombination nodules. We prepared synaptonemal complex (SC) spreads from 124 spermatocytes of three male dogs and mapped 4959 MLH1 foci along 4712 autosomes. The mean number of MLH1 foci for all autosomes was 40.0 foci per cell. Total recombination length of the male dog autosomal genome map was estimated as 2000 cM. A global pattern of MLH1 foci distribution along the autosomal bivalents was rather similar to that found in the mammals studied: a high frequency near the telomeres and a low frequency near the centromeres. An obligate MLH1 focus in the X-Y pairing region was usually located very close to Xp-Yq telomeres. The distances between MLH1 foci at autosomal bivalents were consistent with crossover interference. A comparison of the interference estimates coming from the distribution of MLH1 interfocus distances and RAD51/MLH1 focus ratio indicated a substantial variation between species in the strength of interference.

Abbreviations

ACA	anti-centromere antibody
ANOVA	analysis of variance
BSA	bovine serum albumin
cM	centimorgan
DAPI	4′,6-diamidino-2-phenylindole
Cy3	orange fluorescing cyanine
FITC	fluorescein isothiocyanate
FNa	diploid number of autosomal arms
MLH1	homologue of prokaryotic mutL 1 mismatch repair protein
PBS	phosphate-buffered saline
RAD51	eukaryotic homologue of the prokaryotic RecA protein
SC	synaptonemal complex
SCP3	synaptonemal complex protein 3
SD	standard deviation

Introduction

Meiotic recombination plays a critical role in evolution: it increases genetic and phenotypic variation by creating new potentially beneficial combinations of alleles and prevents mutation meltdown of the genome by removing deleterious mutations. Studies

on various species of mammals demonstrated a wide variation in recombination rates between individuals, population and species (Pardo-Manuel de Villena & Sapienza 2001, Lynn *et al*. 2002, 2004, Jensen-Seaman *et al*. 2004, Coop & Przeworski 2007). Interspecies comparisons are of special interest in view of a long-running discussion about the costs and benefits of recombination (Otto & Lenormand 2002).

Overall recombination rate can be estimated genetically as the total length of the genetic map or cytologically via chiasma count. Genetic maps are constructed on the basis of linkage studies which require large sets of well-controlled crosses or well-characterized pedigree records. This approach provides precise estimates of recombination even between closely linked genes. However, it usually yields biased estimates of the total length of the genetic map. On one hand, summing up of short intervals between the markers leads to overestimation of the total length of chromosome and genome maps. On the other hand, the total length can be underestimated owing to the lack of markers in some chromosome regions (especially near the telomeres). Chiasma counts at diakinesis might provide an unbiased estimate of the total rate of recombination. However, the efficiency of this approach is limited by difficulties in obtaining samples from the appropriate meiotic stage and in measuring the position of chiasmata accurately.

Recently, a new method of cytological recombination mapping has been developed. It is based on immunolocalization of MLH1, a mismatch repair protein of mature recombination nodules, at the synaptonemal complexes (SC) (Anderson *et al*. 1999, Froenicke *et al*. 2002, Koehler *et al*. 2002, Lynn *et al*. 2002). This approach has proved to give reliable estimates of the total recombination rate, as well as the frequency and distribution of recombination events in individual chromosomes. So far, it has been applied to four species of mammals: humans (Lynn *et al*. 2002, Sun *et al*. 2004, 2006a), mouse (Anderson *et al*. 1999, Froenicke *et al*. 2002, Koehler *et al*. 2002), domestic cat (Borodin *et al*. 2007) and common shrew (Borodin *et al*. 2008).

The cytological and genetic studies demonstrated that distribution of recombination sites along meiotic chromosomes is not random and depends on numerous factors including chromosome size, morphology, the GC/AT ratio, and others (Froenicke *et al*. 2002, Sun *et al*. 2004, Jensen-Seaman *et al*. 2004, Borodin *et al*. 2008). Crossovers occurring in the same bivalent usually interfere, i.e. the occurrence on a crossover usually decreases the probability that another will occur close by. This phenomenon is called chiasma interference. It makes a substantial contribution to non-random distribution of crossover along the bivalents (Jones 1987).

Chiasma interference was first described by J.B.S. Haldane (1931) and then studied extensively by such pioneers of cytogenetics as Mather (1938), Callan (1949), Rhoades (1955), and Carpenter (1988). Yet its underlying mechanisms remain unknown (Jones & Franklin 2006). Several modern models link interference with the repair pathway of double-strand DNA breaks occurring at the beginning of meiotic prophase resulting in crossover or non-crossover. The smaller the fraction of those repaired by crossover pathway, the stronger the interference (McPeek & Speed 1995, Bishop & Zickler 2004, Stahl *et al*. 2004, Baudat & de Massy 2007). Immunolocalization of the proteins involved in early stages of chromosome pairing and recombination may provide an estimate of the number of crossing-over precursors. RAD51 is of special interest. It binds single-strand DNA to form nucleoprotein filaments that undergo pairing with duplex DNA (Shinohara & Shinohara 2004) and therefore RAD51 foci at leptotene can be considered as rough markers of the crossing-over precursor sites (Baudat & de Massy 2007).

We used MLH1 and RAD51 immunolocalization to analyze meiotic recombination in the domestic dog (*Canis familiaris*). The diploid chromosome number (2n) of the dog is 78, being one of the highest among mammals. All the autosomes are acrocentric, while the sex chromosomes are bi-armed (Pathak *et al*. 1982). This species is widely used in comparative genomic studies (Wayne & Ostrander 2007). The results of reciprocal painting of dog and human chromosomes show that the dog karyotype is one of the most significantly rearranged karyotypes in mammals: 22 human autosomal paints marked 73 homologous regions on 38 canine autosomes and 38 dog autosomes paints detected 90 homologous segments in the human genome (Yang *et al*. 1999, Sargan *et al*. 2000). Great progress is being achieved in physical and genetic mapping of dog chromosomes (Neff *et al*. 1999, Breen *et al*. 1999, 2004, Guyon

et al. 2003). Finally, a high-quality draft sequence of the dog genome is now available (Lindblad-Toh *et al*., 2005).

In this paper we present cytological estimates of the total length of the genetic map of male dogs and distribution of crossing over along the bivalents. We also estimate crossover interference by the characteristics of distribution of distances between MLH1 foci and RAD51/MLH1 focus ratio.

Material and methods

Spreading and immunostaining

The testes were obtained from three 3-month-old stray male dogs during routine castration. Spermatocyte spreads were prepared from both left and right testes using the technique of Peters *et al*. (1997).

To identify mature recombination nodules, immunostaining of MLH1 was performed as follows. The slides were incubated overnight at 37°C with a rabbit polyclonal antibody against human lateral element protein SCP3 (Abcam, Cambridge, UK) diluted to a concentration of 1:500, a mouse monoclonal antibody to human mismatch repair protein MLH1 (1:30, Pharmingen, San Diego, CA, USA), and a human anti-centromere antibody (ACA) (1:200, Antibodies Inc, Davis, CA, USA) in 3% bovine serum albumin (BSA) in phosphate-buffered saline (PBS). Slides were washed in 1× PBS and incubated for 40 min at 37°C with goat anti-rabbit Cy3-conjugated antibodies (1:500, Jackson, West Grove, PA, USA), goat anti-mouse FITC-conjugated antibodies (1:100, Jackson), and goat anti-human FITC-conjugated antibodies (1:200, Vector Laboratories, Burlingame, CA, USA). Slides were washed with PBS, rinsed briefly with distilled water, dried and mounted in Vectashield with DAPI (Vector Laboratories) to stain DNA and reduce fluorescence fading.

To estimate the number of crossing-over precursor sites in leptotene cells, immunostaining of RAD51 was performed as follows. Slides were first incubated overnight at 37°C with a rabbit polyclonal anti-human RAD51 antibody (1:1000, Calbiochem, San Diego, CA, USA), followed by detection with fluorescein isothiocyanate (FITC)-conjugated goat anti-rabbit IgG antibody (1:500, Jackson) for 1 h. After rinsing, the slides were incubated overnight with a rabbit antibody against SCP3. This primary antibody was detected with donkey anti-rabbit Cy3 (1:500, Jackson) for 1 h.

The preparations were analyzed with an Axioplan 2 Imaging microscope (Carl Zeiss, Jena, Germany) equipped with a CCD camera (CV M300, JAI Corporation, Japan), CHROMA filter sets and ISIS4 image-processing package (MetaSystems GmbH, Altlussheim, Germany). Brightness and contrast of all the images were enhanced using PaintShopPro 7.0.

Measurement and analysis

MLH1 foci were analyzed in pachytene cells with all bivalents completely paired (Figure 1). RAD51 foci were counted in leptotene cells in which the axial elements of SC were already visible, but not paired (Figure 2). Only cells containing complete sets of chromosomes were analyzed. The centromere position for each SC in the pachytene cells was identified by an ACA focus. Although we used the same fluorochrome for detection of the ACA and MLH1 antibodies, ACA foci differed from MLH1 foci by their brighter and more diffuse staining (Figure 1). MLH1 and RAD51 signals were scored only if they were localized on a SC. The length of the SC of each bivalent was measured in micrometers using MicroMeasure 3.3 (Reeves 2001) and the positions of MLH1 foci in relation to the centromere were recorded.

After measurement, autosomal bivalents in each cell were ranked in sequence of decreasing relative length from 1 to 38. There was a continuous gradation in the size of bivalents and only bivalent 1 could be identified unequivocally (Table 1). We therefore divided the remaining bivalents into five classes that included SCs of similar length (SCs 2–7, 8–16, 17–24, 25–31 and 32–38). Each SC was divided into 10 equal-length intervals, and MLH1 distributions were obtained by summing the number of foci in each interval for SCs in the same length class (Figure 3).

In order to estimate interference we measured the absolute distances between neighboring MLH1 foci at the bivalents 1–7 containing two foci. The relative distances between the foci were calculated as fractions of the bivalent length. The distances were fitted to gamma distributions by a maximum-likelihood

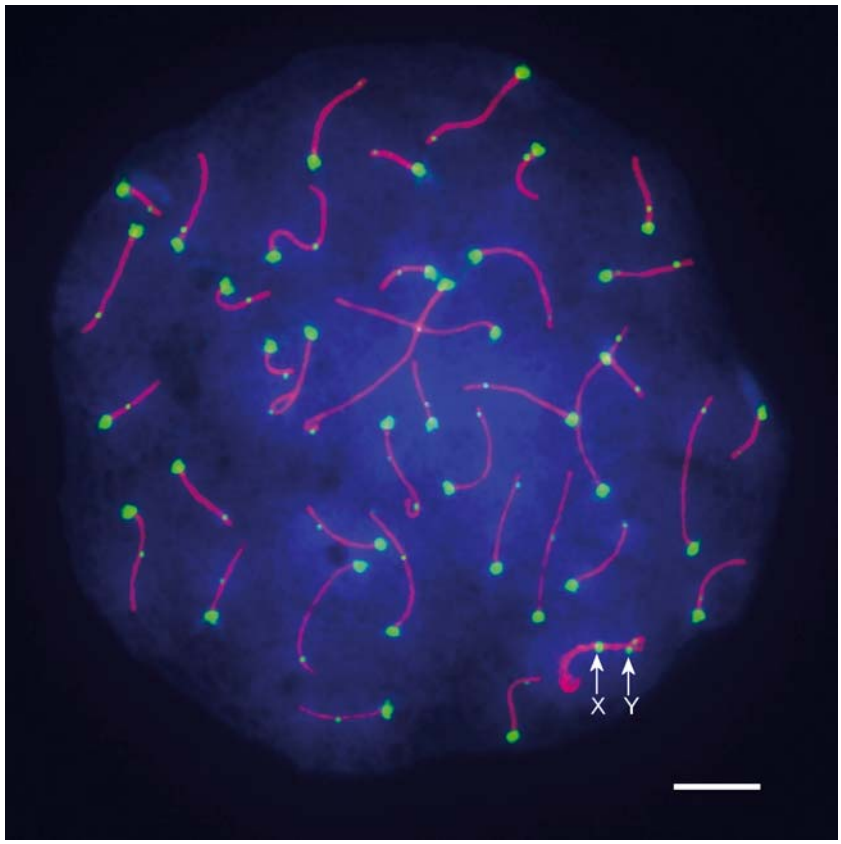

Figure 1. Spread from a dog spermatocyte at pachytene, stained with DAPI (blue) and immunolabeled with antibodies to SCP3 (red), MLH1 (green) and centromere proteins (green). Centromeres differ from MLH1 foci by their brighter and more diffuse staining. Arrows indicate centromeres of X and Y chromosomes. Bar represents 5 μm.

method using Wessa (2008) Free Statistics Software, version 1.1.22-r4 (http://www.wessa.net) and the shape parameter (ν) was used as a measure of the strength of interference (de Boer *et al*. 2006). The STATISTICA 6 package was used for ANOVA, correlations and other statistical analyses.

Results

Characteristics of the autosomal bivalents

The mean (±SD) total length of the autosomal SCs was 246.0 ± 21.5 μm, varying between 194 and 307 μm. This is in a good correspondence with the data obtained by Peterson *et al*. (1994) using a different spreading technique: 212.0 ± 20.0 μm, with a range 188–231 μm. ANOVA revealed significant inter-individual variation in this trait ($F_{2,121} = 13.1$, $p < 0.001$). Significant differences between individuals have also been found in studies on humans (Lynn *et al*. 2002, Sun *et al*. 2004, 2005, 2006a, b) and the common shrew (Borodin *et al*. 2008).

The mean (±SD) number of MLH1 foci for all autosomes was 40.0 ± 1.4 foci per cell, with a range of 36–44. This is in good agreement with an earlier chiasma count in seven diakinesis cells of dogs: 42.6 ± 2.4 (Wada & Imai 1995). We found no differences in number of MLH1 foci per cell between individuals ($F_{2,121} = 0.4$, $p = 0.69$).

To estimate in centimorgans (cM) the recombination length of the autosomal part of the male dog genome, we multiplied the average number of MLH1 foci per cell by 50 map units (one recombination event = 50 cM), which gave 2000 cM.

Altogether, 4712 autosomal SCs were analyzed. Of these, 23 (0.5%) lacked an MLH1 focus. This frequency is within the limits of variation found in

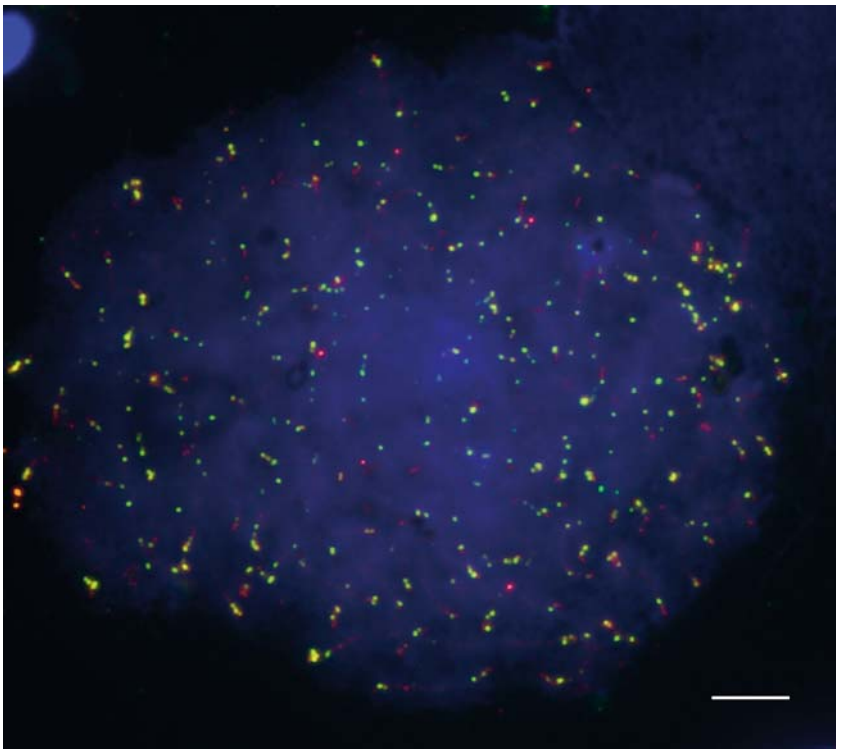

Figure 2. Spread from a dog spermatocyte at leptotene, stained with DAPI (blue) and immunolabeled with antibodies to SCP3 (red), and RAD51 (green). Bar represents 5 μm.

studies on humans (0.3%, Sun *et al*. 2006b), mice (4%, Anderson *et al*. 1999; 1%, Koehler *et al*. 2002) and shrews (0.7%, Borodin *et al*. 2008). The studies on these species demonstrate that small bivalents suffer a much higher risk of recombination failure than large bivalents. All dog chromosomes but the first (for which we did not find achiasmatic bivalents) form SCs comparable in their lengths with human bivalents 13–22. We found the achiasmatic condition among bivalents of various size ranks (Table 1). The cells containing achiasmatic bivalents did not appear to be exceptional (e.g. at late pachytene or poorly stained) and did not differ significantly from the whole sample in their total SC length (240.7 ± 26.4 μm, $t_{140} = 0.9$, $p = 0.35$).

The correlation between the total length of SCs and the number of MLH1 foci per cell was rather weak in male dogs ($r = 0.19$, $p < 0.05$) as well as in male mice, cats and shrews (Froenicke *et al*. 2002, Borodin *et al*. 2007, 2008), in contrast to the strong correlation found in human males (Lynn *et al*. 2002).

Characteristics of the XY bivalent

The X and Y chromosomes of the dog are bi-armed. The mean (±SD) size of the Yq SC was 1.3 ± 0.3 μm. We observed pairing between the tip of Xp and almost the whole Yq (Figure 1). This is in a good agreement with the localization of the pseudoautosomal region at the dog sex chromosomes established by the use of DNA probes (Toder *et al*. 1997, Olivier *et al*. 1999). In 30% of pachytene cells, synapsis extended beyond the Y centromere and, in 10%, both arms of the Y chromosome were synapsed with Xp. On average, the synaptic region involved 60% of Yq.

We detected a single MLH1 focus in the X-Y pairing region in all cells (Figure 1). It was usually located very close to Xp-Yq telomeres. The average distance between the telomeres and the MLH1 focus was 0.3 ± 0.2 μm, ranging from 0 to 0.6 μm. There was a significant positive correlation between the fraction of Xq involved in synapsis and the relative distance of MLH1 foci from the telomere ($r = 0.38$, $p < 0.05$).

Table 1. Length of synaptonemal complex (SC) and number of MLH1 foci per bivalent

Bivalent rank	Absolute length of SC (μm)		Relative length of SC (%)		No. of MLH1 foci		No. of cells containing			
	Mean	SD	Mean	SD	Mean	SD	0 foci	1 focus	2 foci	3 foci
1	13.96	1.59	5.68	0.42	1.67	0.49	0	42	81	1
2	11.50	1.46	4.68	0.36	1.14	0.37	0	108	15	1
3	10.63	1.25	4.31	0.28	1.24	0.47	1	93	29	1
4	10.05	1.13	4.08	0.19	1.12	0.37	2	105	17	0
5	9.62	1.09	3.92	0.18	1.13	0.36	1	106	17	0
6	9.26	0.97	3.78	0.15	1.16	0.39	1	102	21	0
7	8.97	0.90	3.66	0.15	1.10	0.30	0	112	12	0
8	8.66	0.85	3.52	0.16	1.02	0.20	1	119	4	0
9	8.40	0.83	3.40	0.15	1.07	0.26	0	115	9	0
10	8.14	0.75	3.30	0.13	1.02	0.15	0	121	3	0
11	7.91	0.69	3.21	0.10	1.02	0.18	1	120	3	0
12	7.70	0.67	3.12	0.09	1.05	0.22	0	118	6	0
13	7.49	0.65	3.05	0.10	1.03	0.18	0	120	4	0
14	7.25	0.64	2.95	0.10	1.02	0.15	0	121	3	0
15	6.93	0.66	2.83	0.11	1.01	0.16	1	121	2	0
16	6.66	0.63	2.72	0.12	1.04	0.20	0	119	5	0
17	6.44	0.62	2.64	0.13	1.01	0.16	1	121	2	0
18	6.23	0.59	2.54	0.14	1.02	0.15	0	121	3	0
19	6.04	0.55	2.45	0.14	1.01	0.20	2	119	3	0
20	5.83	0.53	2.35	0.12	1.02	0.20	1	119	4	0
21	5.67	0.48	2.29	0.09	1.00	0.18	2	120	2	0
22	5.54	0.48	2.24	0.09	1.00	0.00	0	124	0	0
23	5.40	0.46	2.19	0.09	1.02	0.15	0	121	3	0
24	5.29	0.45	2.15	0.08	0.99	0.09	1	123	0	0
25	5.16	0.43	2.09	0.07	1.00	0.00	0	124	0	0
26	5.04	0.43	2.05	0.07	1.01	0.09	0	123	1	0
27	4.90	0.43	2.00	0.07	1.02	0.13	0	122	2	0
28	4.74	0.45	1.93	0.08	1.00	0.13	1	122	1	0
29	4.55	0.44	1.86	0.09	1.02	0.15	0	121	3	0
30	4.31	0.41	1.77	0.11	1.02	0.18	1	120	3	0
31	4.13	0.41	1.69	0.11	1.00	0.00	0	124	0	0
32	3.95	0.37	1.62	0.13	1.01	0.09	0	123	1	0
33	3.77	0.36	1.54	0.14	1.01	0.09	0	123	1	0
34	3.60	0.35	1.47	0.14	1.00	0.13	1	122	1	0
35	3.42	0.32	1.38	0.13	0.99	0.20	3	119	2	0
36	3.23	0.31	1.30	0.11	1.00	0.00	0	124	0	0
37	2.96	0.34	1.19	0.11	0.99	0.09	1	123	0	0
38	2.67	0.32	1.08	0.10	1.00	0.13	1	122	1	0

Distribution of MLH1 foci along the bivalents

Figure 3 shows distribution of MLH1 foci along bivalents grouped by their size rank. The bivalent 1 demonstrated bimodal distribution with a major peak near the distal end and the other peak in the proximal half of the bivalent. The large bivalents (2–7) also showed peaks at the distal ends, but the distribution of MLH1 foci along the arms of these bivalents was rather flat. In other groups of bivalents (8–38) we observed a gradual decrease of MLH1 foci frequency from telomere to centromere. Thus, all bivalents showed pronounced peaks of MLH1 foci at distal ends and a paucity of them near the centromeres. Almost all MLH1 foci that we observed near the centromeres of the large bivalents were found in those containing two MLH1 foci. Apparently they marked ‘the second crossovers’ that were pushed toward the centromere by the interference of ‘the first crossovers’ that occurred in distal regions.

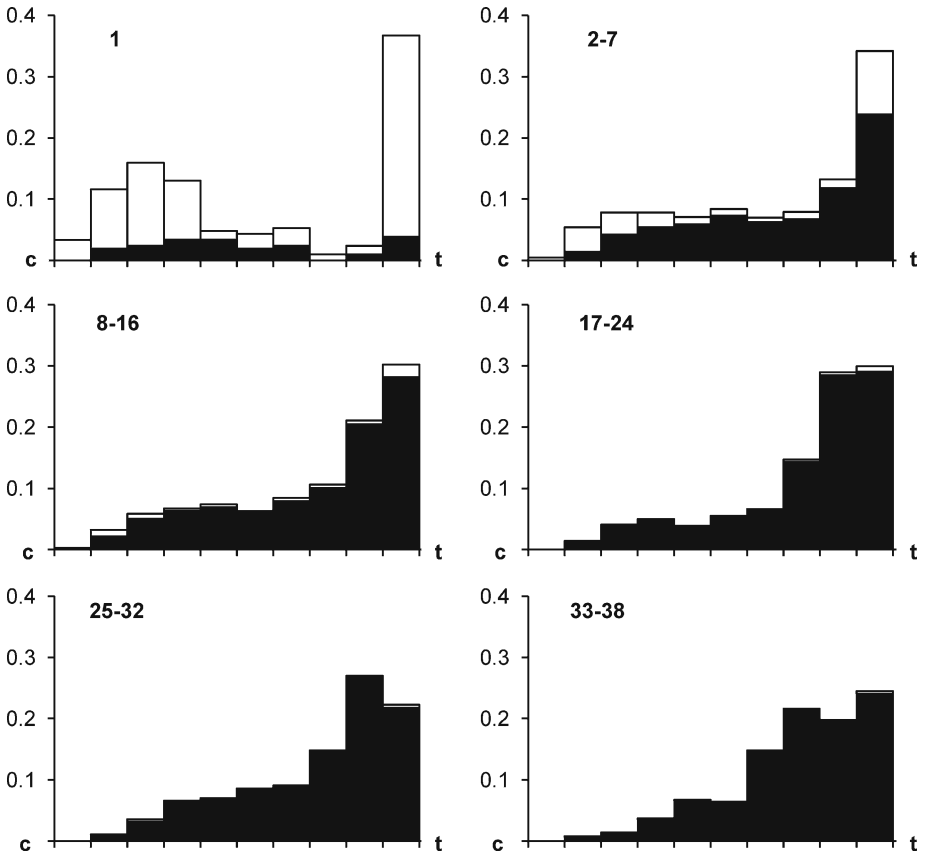

Figure 3. Distribution of MLH1 foci on autosomal SCs from dog spermatocytes. The SCs are divided into groups based on length. The SC size ranks included in each group are indicated in top left corners of the graphs. The *x*-axis shows the position of MLH1 foci in relation to centromere (c) and telomere (t), the marks on this axis are separated by 0.1 of the SC length. The *y*-axis indicates the frequency of MLH1 foci in each 0.1 SC interval. Stacked columns show the frequency for the bivalents containing MLH1 foci in each interval; black columns indicate bivalents with a single MLH1 focus; the white columns those with two MLH1 foci.

Interference

Interference makes a substantial contribution to the determination of recombination patterns of chromosomes. The strength of interference can be estimated from the distances between adjacent recombination sites. In the absence of interference an average distance between neighboring sites at the chromosome containing two crossovers should be around 33% of the chromosome length (Carpenter 1988).

Average relative distances between adjacent MLH1 foci in the bivalents 1 to 7 containing two foci ($N = 115$) was $60 \pm 22\%$ of the bivalent length (range 8–90%). Thus, it was twice that expected in the absence of interference. Overlapping estimates of mean distance between MLH1 foci were obtained in analyses of other mammals (Table 2).

Recently de Boer *et al*. (2006, 2007) suggested estimating the strength of crossover interference using parameters of the gamma distribution. This distribution describes the probability of the distances that would occur if MLH1 focus precursors were randomly placed along the bivalent and only every *n*-th precursor would result in a focus. The higher the *n* value the stronger the interference. The *n* value can be estimated via the shape parameter (ν) of a gamma distribution. We determined the ν value for which the observed frequency distribution of interfocus distances fitted best to a gamma distribution. The ν value estimated for the bivalents 1 to 7 was 6.5 ± 0.6. It is less than the ν values estimated for the chromosome arms of the male common shrew (11–16, Borodin *et al*. 2008) and the mouse (8.9–11.7, de Boer *et al*. 2007), and larger than this parameter for the cat

Table 2. Recombination characteristics of the mammals studied by MLH1 immunolocalization

Species	2n	FNa	Total SC length (μm)	Total number of MLH1 foci	Average interfocus distance in the arms containing two MLH1 foci (% of the arm length)	Reference
Shrew	21–25	40	142.8	21.9	42–55	Borodin *et al.* (2008)
Mouse	40	38	163.7	22.9	70	Froenicke *et al.* (2002)
Cat	38	68	195.3	42.5	47	Borodin *et al.* (2007)
Dog	78	76	246.0	40.0	60	This paper
Man	46	78[a]	297.9	49.8	68	Sun *et al.* (2004)

2n = diploid chromosome number.
FNa = diploid number of autosomal arms.
[a]Sun *et al.* (2004) demonstrated that MLH1 foci occurred very rarely on the short arms of chromosomes 13, 14, 15, 22, and never at 21p; therefore, these arms were not included in FNa.

chromosomes (3.7, Borodin *et al.* 2007). This shows that mammals vary in the strength of interference.

Within the framework of the counting hypothesis of interference (McPeek & Speed 1995, Stahl *et al.* 2004) this value means that, on average in the dog meiosis, every 6th–7th precursor results in a crossover. Thus, the average number of crossing-over precursor sites can be estimated as the average number of MLH1 foci multiplied by 6.5, i.e. as 264 sites per genome. To assess the validity of this estimate, we counted the number of RAD51 foci in 20 leptotene cells of the dogs studied (Figure 2). The mean (±SD) number of these foci was 261.4 ± 57.8. Thus, our estimate of the average number of precursors per genome coming from fitting the distribution of MLH1 interfocus distances to a gamma distribution was rather close to the number of RAD51 foci in leptotene cells. A similar correspondence between interference estimates based on RAD51/crossover ratio (9, Baudat & de Massy 2007) and shape parameter of a gamma distribution (8.9–11.7, de Boer *et al.* 2007) was observed in male mice. These results are in favor of the counting hypothesis of interference.

Discussion

Application of immunostaining techniques to the analysis of recombination in domestic dogs allowed us to estimate the overall recombination rate in this species and describe a general pattern of crossover distribution along the bivalents.

Recombination rate

We estimated the total recombination length of the male dog autosomal genome map as 2000 cM. This is very close to the estimate coming from meiotic linkage analysis: 2054 cM (Breen *et al.* 2004). However, the significance of this similarity should not be overestimated. The dog linkage map is sex-averaged, while it is known that recombination rate in female mammals is usually higher than in males (Burt *et al.* 1991). The overall length of the linkage map is calculated by summing up the short intervals between genetic markers, and is therefore overestimated. Some chromosomes are incompletely mapped owing to a lack of terminal markers and have genetic map lengths smaller than 50 cM (Breen *et al.* 2004).

MLH1 mapping is free of these limitations and provides a more precise estimate of the total recombination length of the male dog genome, which can be used in comparative studies.

To date, the number and distribution of MLH1 foci have been studied in five species of mammals (Table 2). They differ in the total number of crossovers per cell and recombination rate. The autosomal part of the dog genome is 2631 Mb (Sargan *et al*. 2000); thus 1 cM of its genetic map is equal to approximately 1.32 Mb of DNA sequence. This is rather close to the estimates obtained by MLH1 mapping for human males (1.20, Sun *et al*. 2006a) and male cats (1.38, Borodin *et al*. 2007) but about half that for male mice (2.25, Anderson *et al*. 1999) and the males of the common shrew (2.6, Borodin *et al*. 2008).

Chromosome morphology (acrocentrics versus bi-armed chromosomes) may affect the total number of crossovers. Bidau *et al*. (2001) and Dumas & Britton-Davidian (2002) showed a significant decrease in recombination frequency in the arms of metacentric chromosomes compared with twin acrocentrics of the house mouse. However, this is not always the case. Borodin *et al*. (2008) did not find a significant difference between acrocentric and metacentric homozygotes in the common shrew. Nor does interspecies comparison indicate a substantial effect of chromosome morphology. Dogs have all acrocentric autosomes, while most human and cat autosomes are bi-armed; yet all three species are similar in recombination rate.

The species with high recombination rate (human, cat and dog) have higher numbers of autosomal arms in the karyotype, or fundamental number (FNa), and larger length of SC than those with low recombination rate (mouse and shrew). A strong positive correlation between FNa and chiasma count has been already demonstrated (Pardo-Manuel de Villena & Sapienza 2001, and references herein). This correlation is based on the requirement of at least one chiasma per arm for proper chromosome segregation (Jones 1984; Jones & Franklin 2006). Thus, FNa/2 would determine the lower limit of crossover number per cell. Another important factor controlling recombination rate is a total SC length. This is positively correlated with crossover frequency (Peterson *et al*. 1994, Kleckner *et al*. 2003). Long bivalents may accommodate more than one chiasma.

The number of multiple crossovers per chromosome arm is restricted by crossover interference. Therefore, interference may be considered as a factor controlling the upper limit of the recombination rate (Falque *et al*. 2007). A comparison of the interference estimates coming from the distribution of MLH1 interfocus distances and RAD51/MLH1 focus ratio indicates a substantial difference between species in the strength of interference. We suppose that this factor may contribute to interspecies difference in recombination rate. For example, cats have smaller FNa, smaller total SC length, but weaker interference than do dogs (Table 2), and they exceed dogs in the average number of MLH1 foci ($t_{178} = 15.4$, $p < 0.001$).

Individual variation in the strength of interference has been detected in humans (Broman & Weber 2000) and is likely to be present in other species. Selective changes of this parameter may serve as a mechanism of adaptive 'fine adjustment' of recombination rate, additionally or alternatively to 'coarse adjustment' achieved by fixation of the chromosome rearrangements that change FNa, such as pericentric inversions, tandem fusions and centromere shifts.

Crossover distribution

Analyzing MLH1 foci distribution along the dog bivalents, we found a high frequency of the foci near the telomeres and a low frequency near the centromeres. This is very similar to the pattern observed in other mammals studied: mice (Anderson *et al*. 1999, Froenicke *et al*. 2002), humans (Lynn *et al*. 2002, Sun *et al*. 2004, 2006a), shrews (Borodin *et al*. 2008), and cats (Borodin *et al*. 2007).

An excess of recombination near the telomeres is apparently determined by their early involvement in chromosome alignment and pairing (Scherthan *et al*. 1996, Zickler & Kleckner 1999, Brown *et al*. 2005). The farther from the telomere the chromosome region is located, the lower the probability of its involvement in recombination. This also explains, at least partially, a relative paucity of single MLH1 foci near the centromeres in the majority of the dog bivalents.

Low frequency of MLH1 foci near the centromeres has been also observed in mouse and human bivalents. It was interpreted as an indication of suppressive effect of centromeric heterochromatin on recombination (Anderson *et al*. 1999, Froenicke *et al*. 2002). This effect is unlikely to play an important role in MLH1 focus distribution along the dog chromosomes, most of which contain a very small amount of C-heterochromatin. Only a few dog

chromosomes have detectible C-blocks (Pathak *et al*. 1982). Subcentromeric suppression of recombination has also been described in the common shrew, another species with a very low content of C-heterochromatin (Borodin *et al*. 2008). On the other hand, MLH1 foci located very close to centromeres (less than 0.5 μm) have been detected in cat chromosomes characterized by prominent C-blocks (Borodin *et al*. 2007). Apparently the recombination suppression near the centromeres is not as tightly linked with the presence of C-heterochromatin as is commonly believed.

Crossover distribution depends on chromosome morphology. Comparing recombination patterns of syntenic regions in the dog and fox chromosomes, Kukekova *et al*. (2007) found that the suppression of recombination in pericentromeric regions of the metacentric fox chromosomes was more pronounced than in the corresponding segments of acrocentric dog chromosomes. A reduction in the number of proximal chiasmata and a more distal chiasma distribution in metacentric homozygotes compared with acrocentric homozygotes was also observed in the house mouse (Bidau *et al*. 2001, Dumas & Britton-Davidian 2002) and the common shrew (Giagia-Athanasopoulou & Searle 2003, Borodin *et al*. 2008) in cases of Robertsonian polymorphism.

This difference in crossover distribution can be attributed to the difference between acrocentric and metacentric chromosomes in the spatial arrangement of their centromeres during leptotene. The centromeres of the acrocentrics are clustered in a restricted area of the nuclear surface by their proximal telomeres, but the centromeres of metacentrics are not (Scherthan *et al*. 1996). Therefore, the chance of pairing initiation and crossover occurrence in proximal regions is higher in acrocentric than in metacentric chromosomes.

Acknowledgements

This work was supported by research grants from the Russian Foundation for Basic Research and the programs of the Russian Academy of Sciences 'Biosphere Origin and Evolution' and 'Biodiversity'. We thank Mrs Marina Rodionova for her help in SC spreading and the Microscopic Center of the Siberian Department of the Russian Academy of Sciences for granting access to microscopic equipment. C.J.B. is especially indebted to CNPq, FAPERJ and FIOCRUZ for supporting his research.

References

Anderson LK, Reeves A, Webb LM, Ashley T (1999) Distribution of crossing over on mouse synaptonemal complexes using immunofluorescent localization of MLH1 protein. *Genetics* **151**: 1569–1579.

Baudat F, de Massy B (2007) Regulating double-stranded DNA break repair towards crossover or non-crossover during mammalian meiosis. *Chromosome Res* **15**: 565–577.

Bidau CJ, Giménez MD, Palmer CL, Searle JB (2001) The effects of Robertsonian fusions on chiasma frequency and distribution in the house mouse (*Mus musculus domesticus*) from a hybrid zone in northern Scotland. *Heredity* **87**: 305–313.

Bishop DK, Zickler D (2004) Early decision: meiotic crossover interference prior to stable strand exchange and synapsis. *Cell* **117**: 9–15.

Borodin PM, Karamysheva TV, Rubtsov NB (2007) Immunofluorescent analysis of meiotic recombination in the domestic cat. *Cell Tissue Biol* **1**: 503–507.

Borodin PM, Karamysheva TV, Belonogova NM *et al*. (2008) Recombination map of the common shrew, *Sorex araneus (Eulipotyphla, Mammalia)*. *Genetics* **178**: 621–632.

Breen M, Langford CF, Carter NP *et al*. (1999) FISH mapping and identification of canine chromosomes. *J Hered* **90**: 27–30.

Breen M, Hitte C, Lorentzen TD *et al*. (2004) An integrated 4249 marker FISH/RH map of the canine genome. *BMC Genomics* **5**: 1–11.

Broman KW, Weber JL (2000) Characterization of human crossover interference. *Am J Hum Genet* **66**: 1911–1926.

Brown PW, Judis L, Chan ER *et al*. (2005) Meiotic synapsis proceeds from a limited number of subtelomeric sites in the human male. *Am J Hum Genet* **77**: 556–566.

Burt A, Bell G, Harvey PH (1991) Sex differences in recombination. *J Evol Biol* **4**: 259–277.

Callan HG (1949) Chiasma interference in diploid, tetraploid and interchange spermatocytes of the earwig, *Forficula auricularia*. *J Genet* **49**: 209–213.

Carpenter ATC (1988) Thoughts on recombination nodules, meiotic recombination, and chiasmata. In: Kucherlapati R, Smith GR, eds. *Genetic Recombination*. Washington, DC: American Society for Microbiology, pp. 529–548.

Coop G, Przeworski M (2007) An evolutionary view of human recombination. *Nat Rev Genet* **8**: 23–34.

de Boer E, Stam P, Dietrich AJJ *et al*. (2006) Two levels of interference in mouse meiotic recombination. *Proc Natl Acad Sci U S A* **103**: 9607–9612.

de Boer E, Dietrich AJJ, Hoog C *et al*. (2007) Meiotic interference among MLH1 foci requires neither an intact axial element structure nor full synapsis. *J Cell Sci* **120**: 731–736.

Dumas D, Britton-Davidian J (2002) Chromosomal rearrangements and evolution of recombination: comparison of chiasma distribution patterns in standard and Robertsonian populations of the house mouse. *Genetics* **162**: 1355–1366.

Falque M, Mercer R, Mézard C *et al.* (2007) Patterns of recombination and MLH1 foci density along mouse chromosomes: modeling effects of interference and obligate chiasmata. *Genetics* **176**: 1453–1467.

Froenicke L, Anderson LK, Wienberg J, Ashley T (2002) Male mouse recombination maps for each autosome identified by chromosome painting. *Am J Hum Genet* **71**: 1353–1368.

Giagia-Athanasopoulou EB, Searle JB (2003) Chiasma localization in male common shrews *Sorex araneus*, comparing Robertsonian trivalents and bivalents. *Mammalia* **67**: 295–299.

Guyon R, Lorentzen TD, Hitte C *et al.* (2003) A 1-Mb resolution radiation hybrid map of the canine genome. *Proc Natl Acad Sci U S A* **100**: 5296–5301.

Haldane JBS (1931) The cytological basis of genetic interference. *Cytologia* **3**: 54–65.

Jensen-Seaman MI, Furey TS, Payseur BA *et al.* (2004) Comparative recombination rates in the rat, mouse, and human genomes. *Genome Res* **14**: 528–538.

Jones GH (1984) The control of chiasma distribution. *Symp Soc Exp Biol* **28**: 293–320.

Jones GH (1987) Chiasmata. In: Moens PB, ed. *Meiosis*. New York: Academic Press, pp. 213–244.

Jones GH, Franklin FC (2006) Meiotic crossing-over: obligation and interference. *Cell* **126**: 246–248.

Kleckner N, Storlazzi A, Zickler D (2003) Coordinate variation in meiotic pachytene SC length and total crossover/chiasma frequency under conditions of constant DNA length. *Trends Genet* **19**: 623–628.

Koehler KE, Cherry JP, Lynn A *et al.* (2002) Genetic control of mammalian meiotic recombination. I. Variation in exchange frequencies among males from inbred mouse strains. *Genetics* **162**: 297–306.

Kukekova AV, Trut LN, Oskina IN *et al.* (2007) A meiotic linkage map of the silver fox, aligned and compared to the canine genome. *Genome Res* **17**: 387–399.

Lindblad-Toh K, Wade CM, Mikkelsen TS *et al.* (2005) Genome sequence, comparative analysis and haplotype structure of the domestic dog. *Nature* **438**: 803–819.

Lynn A, Koehler KE, Judis L *et al.* (2002) Genetic length of mammalian genomes: inter-individual variation and dependence on synaptonemal complex length. *Science* **296**: 2222–2225.

Lynn A, Ashley T, Hassold T (2004) Variation in human meiotic recombination. *Annu Rev Genomics Hum Genet* **5**: 317–349.

Mather K (1938) Crossing-over. *Biol Reviews* **13**: 252–292.

McPeek MS, Speed TP (1995) Modeling interference in genetic recombination. *Genetics* **139**: 1031–1044.

Neff MW, Broman KW, Mellersh CS *et al.* (1999) A second-generation genetic linkage map of the domestic dog, *Canis familiaris*. *Genetics* **151**: 803–820.

Olivier M, Breen M, Binns MM, Lust G. (1999) Localization and characterization of nucleotide sequences from the canine Y chromosome. *Chromosome Res* **7**: 223–233.

Otto SP, Lenormand T (2002) Resolving the paradox of sex and recombination. *Nat Rev Genet* **3**: 252–361.

Pardo-Manuel de Villena F, Sapienza C (2001) Recombination is proportional to the number of chromosome arms in mammals. *Mamm Genome* **12**: 318–322.

Pathak S, Tuinen PV, Merry DE (1982) Heterochromatin, synaptonemal complex, and NOR activity in the somatic and germ cells of a male domestic dog, *Canis familiaris* (Mammalia, Canidae). *Cytogenet Cell Genet* **34**: 112–118

Peters AH, Plug AW, van Vugt MJ, de Boer P (1997) A drying-down technique for the spreading of mammalian meiocytes from the male and female germline. *Chromosome Res* **5**: 66–68.

Peterson DG, Stack SM, Healy JL *et al.* (1994) The relationship between synaptonemal complex length and genome size in four vertebrate classes (Osteicthyes, Reptilia, Aves, Mammalia). *Chromosome Res* **2**: 153–162.

Reeves A (2001) Micromeasure: a new computer program for the collection and analysis of cytogenetic data. *Genome* **44**: 439–443.

Rhoades MM (1955) Meiosis in maize. *J Hered* **41**: 58–67.

Sargan DR, Yang F, Squire M *et al.* (2000) Use of flow-sorted canine chromosomes in the assignment of canine linkage, radiation hybrid, and syntenic groups to chromosomes: refinement and verification of the comparative chromosome map for dog and human. *Genomics* **69**: 182–195.

Scherthan H, Weich S, Schwegler H *et al.* (1996) Centromere and telomere movements during early meiotic prophase of mouse and man are associated with the onset of chromosome pairing. *J Cell Biol* **134**: 1109–1125.

Shinohara A, Shinohara M (2004) Roles of RecA homologues Rad51 and Dmc1 during meiotic recombination. *Cytogenet Genome Res* **107**: 201–207.

Stahl FW, Foss HM, Young LS *et al.* (2004) Does crossover interference count in *Saccharomyces cerevisiae*? *Genetics* **168**: 35–48.

Sun F, Oliver-Bonet M, Liehr T *et al.* (2004) Human male recombination maps for individual chromosomes. *Am J Hum Genet* **74**: 521–531.

Sun F, Trpkov K, Rademaker A, Ko E, Martin RH (2005) Variation in meiotic recombination frequencies among human males. *Hum Genet* **116**: 172–178.

Sun F, Oliver-Bonet M, Liehr T *et al.* (2006a) Variation in MLH1 distribution in recombination maps for individual chromosomes from human males. *Hum Mol Genet* **15**: 2376–2391.

Sun F, Oliver-Bonet M, Liehr T *et al.* (2006b) Analysis of non-crossover bivalents in pachytene cells from 10 normal men. *Hum Reprod* **21**: 2335–2339.

Toder R, Gläser B, Schiebel K *et al.* (1997) Genes located in and near the human pseudoautosomal region are located in the X-Y pairing region in dog and sheep. *Chromosome Res* **5**: 301–306.

Wada MY, Imai HT (1995) Theoretical analyses of chiasmata using a novel chiasma graph method applied to Chinese hamsters, mice, and dog. *Jpn J Genet* **70**: 233–265.

Wayne RK, Ostrander EA (2007) Lessons learned from the dog genome. *Trends Genet* **23**: 557–567.

Wessa P (2008) Maximum-likelihood Gamma Distribution Fitting (v1.0.1) in Free Statistics Software (v1.1.22-r4). Office for Research Development and Education; URL http://www.wessa.net/rwasp_fitdistrgamma.wasp/.

Yang F, O'Brien PC, Milne BS *et al.* (1999) A complete comparative chromosome map for the dog, red fox, and human and its integration with canine genetic maps. *Genomics* **62**: 189–202.

Zickler D, Kleckner N (1999) Meiotic chromosomes: integrating structure and function. *Annu Rev Genet* **33**: 603–754.